Archives of Materials Science and Engineering

Volume 50
Issue 1
July 2011
Pages 43-55

International Scientific Journal
published monthly by the
World Academy of Materials
and Manufacturing Engineering

Sintered stainless steel surface alloyed with Si_3N_4 powder

Z. Brytan*, L.A. Dobrzański, W. Pakieła

Division of Materials Processing Technology, Management and Computer Techniques in Materials Science, Institute of Engineering Materials and Biomaterials, Silesian University of Technology, ul. Konarskiego 18a, 44-100 Gliwice, Poland

* Corresponding author: E-mail address: zbigniew.brytan@polsl.pl

Received 10.04.2011; published in revised form 01.07.2011

ABSTRACT

Purpose: The goal of this study was to investigate effects of laser surface alloying with Si_3N_4 powder on the microstructural changes and properties of vacuum sintered stainless steels, both austenitic X2CrNi17-12-2, ferritic X6Cr13 and duplex X2CrNiMo22-8-2.

Design/methodology/approach: High power diode laser (HPDL) was applied to surface modification of sintered stainless steels with Si_3N_4 powder. The influence of laser alloying conditions on the width, penetration depth of alloyed surface layer were studied and analysed via FEM simulation. The microstructure of alloyed layers was examined using light and scanning electron microscopy as well as X-ray diffraction. The microhardness and wear resistance of studied surface layers were also evaluated.

Findings: The hardness increased with addition of Si_3N_4 due to strong solution hardening effect of nitrogen and silicon that dissolved in the steel matrix during laser alloying. The strong austenite stabilizer effect of nitrogen was observed in ferritic stainless steel that revealed duplex microstructure. The hardness increased with addition of Si_3N_4 due to strong solution hardening effect of nitrogen and silicon dissolved in the steel matrix during laser alloying. The hardening effect of Si_3N_4 was strongest in case of ferritic stainless steel where microhardness increased to 450 HV0.1 for 2.1 kW of laser beam power. The duplex stainless steel shows the regular microhardness on the whole penetration depth. Laser surface alloying with Si_3N_4 improved wear resistance of sintered stainless steels compared to not processed stainless steel as well as comparing layers prepared as machined grooves and surface with pre-coated paste.

Practical implications: Laser surface alloying with Si_3N_4 powder can be an efficient method of surface layer hardening of sintered stainless steels and produce improvement of surface layer properties in terms of hardness and wear resistance. Moreover, application of high power diode laser HPDL and surface prepared as machined grooves can guarantee uniform heating of treated surface, thus uniform thermal cycle across processed area and uniform penetration depth of alloyed surface layer.

Originality/value: Application of high power diode laser can guarantee uniform heating of treated surface, thus uniform thermal cycle across processed area and uniform penetration depth of alloyed surface layer.

Keywords: Laser surface alloying; Sintered stainless steel; Silicon nitride; HPDL

Reference to this paper should be given in the following way:

Z. Brytan, L.A. Dobrzański, W. Pakieła, Sintered stainless steel surface alloyed with Si_3N_4 powder, Archives of Materials Science and Engineering 50/1 (2011) 43-55.

MATERIALS MANUFACTURING AND PROCESSING

1. Introduction

The laser surface alloying (LSA) of stainless steel with pre-coated powder paste or injecting directly powder to the molten pool was investigated by many authors [1-9]. The laser surface treatment can led to the hardening of stainless steel surface layer and produce microstructural changes both alloying with hard particles like carbides TiC, SiC, Cr_3C_2, WC or their compounds like AlSiFe, NiCrSiB, or alloying with nitrides (like Si_3N_4, Si_3N_4+Ti), borides and their mixes or elemental powders like molybdenum that result in the modification of their resistance to pitting, intergranular and stress corrosion cracking.

Tsai et. al [8] studied laser surface alloying applying CO_2 laser of austenitic stainless steel type AISI 316L (X2CrNiMo17-12-2) with silicon nitride pre-coated as gel prepared by mixing Si_3N_4 and polyvinyl alcohol, where the coating thickness was 0.1mm. The surface of stainless steel was alloyed in Si and microstructure of surface layer was composed of the duplex microstructure of austenitic and ferritic phase. However, thickness of hardened surface layer was relatively narrow, about 200μm. The concentration of Si in alloyed layers produced in this study ranged from 2-9% depending on pre-coating thickness, scanning speed and laser beam power. Austenitic stainless steel laser surface alloyed with various pre-coated thickness of Si_3N_4 was found to exhibit increased hardness. The Si_3N_4 was found to undergo decomposition in to Si and N during laser alloying and the increased hardness was strong dependent of Si content in the region. The studies on LSA of carbon steel with powders containing silicon nitride were performed by Sha et. al [9] that examined surface modification by cladding of martensitic stainless steel S42000 (X20Cr13) powder with added silicon nitride Si_3N_4 on a medium carbon steel using WCO_2 laser also showed decomposition of Si_3N_4 during the laser treatment.

The LSA treatment of stainless steel can improve their intergranular, pitting and cavitation erosion resistance as well as wear resistance. Laser surface remelting was successfully applied to restore localized corrosion resistance in sensitized and in cold-worked and sensitised stainless steel. Laser surface allying using High Power Diode Laser (HPDL) is well established method of surface properties improvement for many engineering materials [10-15] and the stainless steel still remain very attractive to develop its surface modification using conventional surface treatment methods as well as thermo-mechanical methods and laser surface treatments [16-21].

Besides conventional stainless steel the alloys produced via powder metallurgy plays an important role in the structural components market, where are mainly applied in automotive industry, household appliances and electromechanical and precision devises. The production of sintered parts form stainless steels is well known and industrialized. The sintered stainless steels are widely used thank to their high corrosion resistance, but due to low hardness their terminological properties are still very weak. Laser surface remelting of powder metallurgy austenitic stainless steel may result in the improvement of overall material properties in surface layer due to density reduction and microstructure refinement, therefore the mechanical and corrosion performance will increase [22, 23].

The present study investigate LSA of sintered stainless steel with Si_3N_4 powder deposited on the sample surface in form of pre-coated paste as well as surface with machined grooves of different number and depth. In presented study austenitic, ferritic and duplex stainless steel was laser alloyed.

2. Experimental procedure

2.1. Substrate material

Three different sintered stainless steels were produced and investigated: austenitic, ferritic and duplex stainless steel with compositions presented in Table 1. For powder preparation the austenitic stainless steel powder 316LHD and ferritic 410LHD of Hoeganes with particle size of <150 μm were used. The duplex sintered stainless steel was obtained by addition of single element powders such as FeCr, Ni, Mo and Cu powder in right quantity to the master alloy of ferritic410LHD powder to obtain the chemical composition similar to duplex one. The manufacturing procedure of sintered stainless steel was well described in the paper [24-26]. During preparation of stainless steel powders the Acrawax was used as a lubricant in the quantity of 0.65 wt.%. Premixes were prepared in Turbula mixer for 20 min. and then uniaxially compacted in specimens of 10×10×55 mm at 700 MPa. The de-waxing process was performed at 550°C for 60 minutes in a nitrogen atmosphere. Samples were then sintered in a vacuum furnace with Ar backfilling at temperature 1250°C for 60 min. During the sintering cycle a solution annealing at 1050°C/1h was done and then the rapid cooling under pressure of 0.6 MPa of nitrogen was applied.

2.2. Laser surface alloying

The laser surface alloying was performed using Rofin DL 020 high power diode laser (HPDL) with rectangular laser beam spot at argon atmosphere with the following laser parameters: radiation wavelength 808±5 nm, beam output power (continuous wave) 2300 W, beam focal length 82/32 mm, laser beam spot dimension 1.8-6.8 mm, power density range in the laser beam plane 0.8-36.5 kW/cm^2. The laser treatment was conduced at 0.7, 1.4 and 2.1 kW of laser beam power and constant scanning speed rate of 0.5 and 0.3 m/min.

The alloyed surface layers on sintered stainless steel were produced as single stringer beads, the laser beam was focused on the top of specimens. The long side of laser beam spot was set perpendicularly to the alloying direction. The laser beam was guided along longer side (55 mm) of specimens, the side compatible with their pressing direction.

The surface of sintered stainless steel was covered with 0.l mm thin layer of Si_3N_4 powder applied on surface in form of paste prepared as a mixture of inorganic sodium glass in proportion 30% glass and 70% Si_3N_4 powder.

Second approach consisted in the special mechanical working of sample surface, where on specimens surface two or three parallel grooves, deep for 0.5 and 1.0 mm of triangular shape (with angle of 45°) were machined. The grooves were located along sample axis and distance between them was ca. 1.0 mm. Such prepared grooves were filled with pure Si_3N_4 powder.

Table 1.
The nominal chemical composition of sintered stainless steels powders used in investigations

Powder designation		Elements concentration, wt.%								
EN 10088 corresponding grade	Manufacturer designation	Cr	Ni	Mo	Si	Mn	C	N	S	Fe
X2CrNiMo17-12-2	316 LHD	16.2	12.3	2.2	0.9	0.10	0.019	0.05	0.006	bal.
X6Cr13	410 LHD	11.9	0.15	-	0.8	0.08	0.009	0.05	0.03	bal.
X2CrNiMo22-8-2	-	22.72	8.10	2.00	0.70	0.60	0.03	-	-	bal.

2.3. Materials characterization

Microstructure observations and geometrical characteristics of weld bead were carried out in the light and scanning electron microscope (SEM) with the EDS probe. Light microscope observations involved etching using Aqua Reggia reagent.

The evaluation of phase composition was made using X-ray diffractometer with the filtered copper or cobalt lamp rays at acceleration voltage of 45 kV and heater current of 40 mA. The measurements were made in diffraction angle from 30 to 130° of 2θ. The X-ray scan was performed parallel to alloying direction.

The Vickers microhardness $HV_{0.1}$was measured on the cross-section of alloyed surface in the FM-AKS 9000 of Future-Techautomated microhardness tester and a depth profile of the microhardness was determined.

Abrasion behaviours have been tested using pin-on-plate method, where hardened steel ball was reciprocally moved along the surface. The wear test was evaluated basing on the confocal images of produced wear track and then wear volume was calculated basing on geometry of wear track. Wear test was performed with fallowing conditions: hardened steel ball diameter 5.0 mm, load during test 7.4 kN, reciprocal sliding movement, path of friction 7 mm, constant 9000 cycles.

3. Results and discussion

The sintered stainless steel shows density of between 7.2-7.3 g/cm^3 and open porosity of about 5% and ca. 92% of theoretical density. The microstructure of austenitic stainless steel prior the laser treatment was composed of austenitic grains with presence of some twinned grains. The ferritic stainless steel shows regular grains of ferrite while duplex microstructure was composed of uniform distributed ferritic and austenitic grains. Applied sintering cycle in vacuum followed be rapid cooling from sintering temperature enabled correct duplex microstructure formation without precipitations of intermetallic phases.

The volume and shape of the melting pool depends largely on the applied laser power and scanning speed. With the increase of laser beam power the width of remelting zone increased (Fig. 1a). When laser beam power is in range of 1.4-2.1 kW the melting width was varied in ranged from 4.7 to 6.4. Application of 0.7 kW laser beam power at scanning speed 0.5 m/min did not caused expected results in terms of penetration depth.

The penetration depth of alloyed layer increased too with higher laser beam power. The greatest penetration depth was obtained for austenitic stainless steel X2CrNiMo17-12-2 (0.9 mm), while for duplex it was ca. 0.35 mm and only 0.2-0.25 for ferritic stainless steel X6Cr13 (Fig. 1b). The authors have been reported in previous works, that sintered austenitic stainless steel remelted in similar conditions shows the penetration depth of maximum 1.0 mm, thus the presence of pre-coated alloying paste on samples surface considerably decreased the maximal possible penetration depth. Pre-coated thin layer (0.1 mm) of Si_3N_4 paste creates a barrier that reduces heat transfer to the steel and thereby reduces the substrate penetration depth. Pre-coated paste reflects laser beam radiation and lowers the penetration depth due to high reflectance loss of the incident laser beam that also depends on the colour and roughness of pre-coated material. Moreover, heat penetration into the sample is decreased due to porosity of the substrate that acts as an insulator.

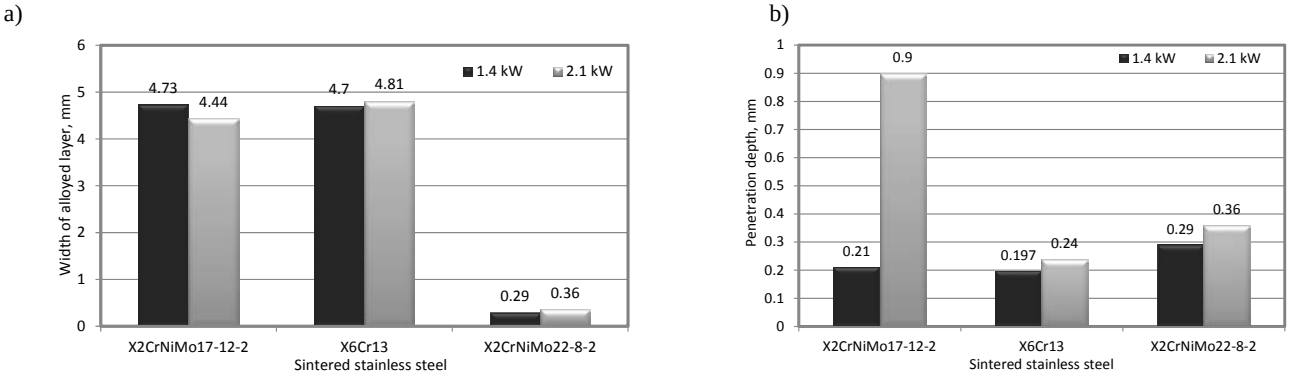

Fig. 1. Geometrical characterization of alloyed layer, a) width and b) penetration depth of surface pre-coated with Si_3N_4 powder paste and laser processed

Surface pre-coated with Si_3N_4 powder after laser remelting shows non-uniform surface topography. Depending on laser conditions surface has non regular remelted zone and only when using high laser energy the surface quality can be acceptable. The cross-sectional views of sintered stainless steels surface layer alloyed with Si_3N_4 powder in form of pre-coated paste were presented in Fig. 2. Generally in aim to obtain properly remelted surface layer, when using pre-coated paste of Si_3N_4 powder at constant scanning speed of 0.5 m/min the laser beam power should be as high as possible, in case of studied conditions only 2.1 kW can guarantee proper surface quality.

The second approach of alloying was based on the surface preparation where one the sample surface two or three grooves where machined with a different depth of 0.5 or1.0 mm. In this case the best results were obtained for machined three groves with depth of 0.5 mm (Fig. 3).

As in the previous approach, the best surface quality and the most optimal penetration depth was obtained when applying laser beam power of 2.1 kW. The second approach uses a slightly slower scanning speed rate 0.3 m/min. The combination of slower scanning speed and high laser beam power of 2.1 kW with the machined grooves filled with Si_3N_4 powder gave much better results than in the case where the sample is covered with pre-coated powder paste as a mixture of water glass and Si_3N_4 powder. In this case the highest penetration depth was observed for duplex stainless steel X2CrNiMo22-8-2 (Fig. 4). Stainless steels surfaces prepared as machined grooves shows higher surface quality than pre-coated with powder. The way of Si_3N_4 deposition on the surface influences the quantity of remelted material and dilution ratio. Regarding the surface quality when Si_3N_4 was deposited as pre-coated paste with increase of laser beam energy indispensable to proper remelting the superficial porosities and large craters where drastically increased (Fig. 5)

This effect was completely eliminated in case of remelting surface with machined grooves filled with Si_3N_4 powder (Fig. 6). The surface of stainless steels after alloying shows silver metallic shine and weld bead of alloyed layer is uniform, flat and smooth without any visible undercuts or superficial cracks (Fig. 6).

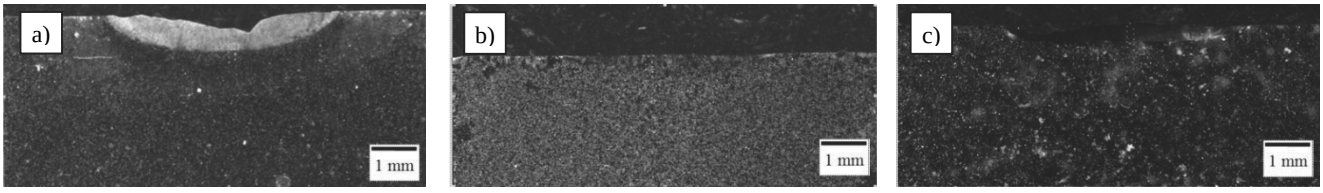

Fig. 2. The surface layer cross section of stainless steel, respectively a) austenitic, b) ferriticand c) duplex stainless steel alloyed with Si_3N_4 powder in form of pre-coated layer at laser beam power of 2.1 kW and scanning speed 0.5 m/min

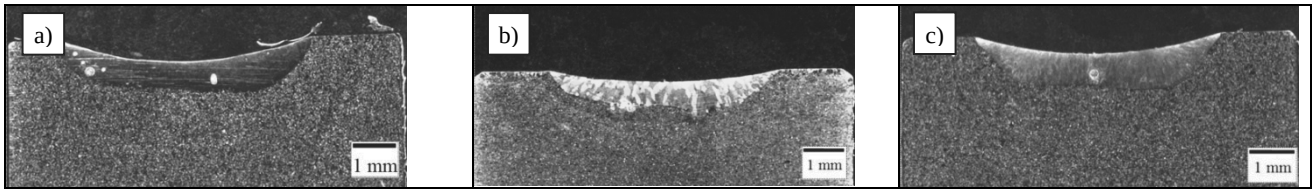

Fig. 3. The surface layer cross section of stainless steel, respectively a) austenitic (3 grooves), b) ferritic (2 grooves) and c) duplex stainless steel (2 grooves) alloyed with Si_3N_4 powder, that filled surface grooves, at laser beam power of 2.1 kW and scanning speed 0.3 m/min

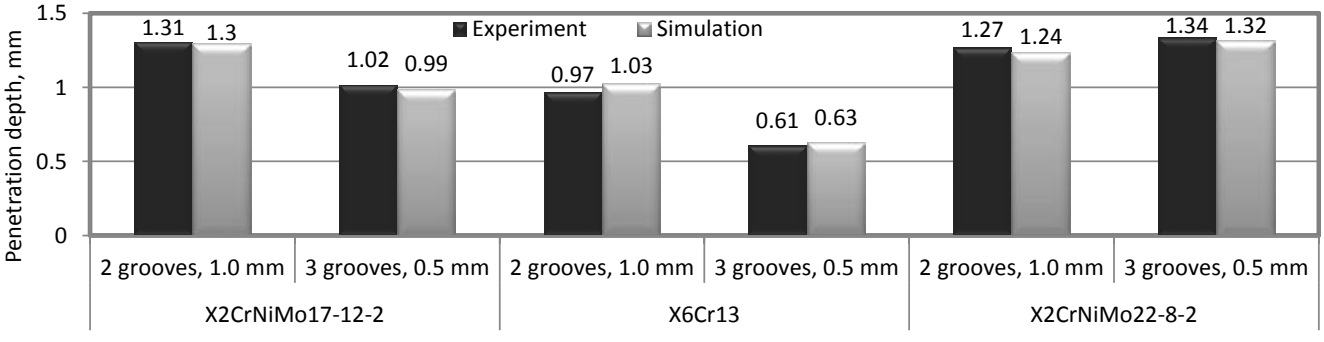

Fig. 4. Comparison of experimental and simulated penetration depth of surface alloyed with Si_3N_4 at laser beam power 2.1 kW, scanning speed 0.3 m/min

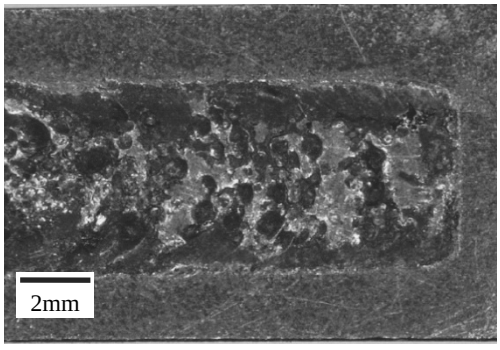

Fig. 5. Surface layer of duplex sintered stainless steel X2CrNiMo22-8-2 alloyed with Si_3N_4 powder in form of pre-coated paste of 0.1 mm, laser beam power 2.1 kW, scanning speed 0.5 m/min

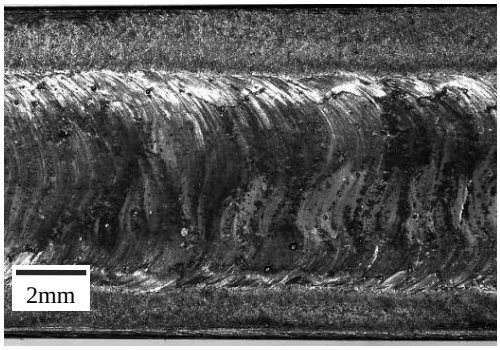

Fig. 6. Surface layer of duplex sintered stainless steel X2CrNiMo22-8-2 alloyed with Si_3N_4 powder, surface with machined 3 grooves of 0.5 mm, laser beam power 2.1 kW, scanning speed 0.3 m/min

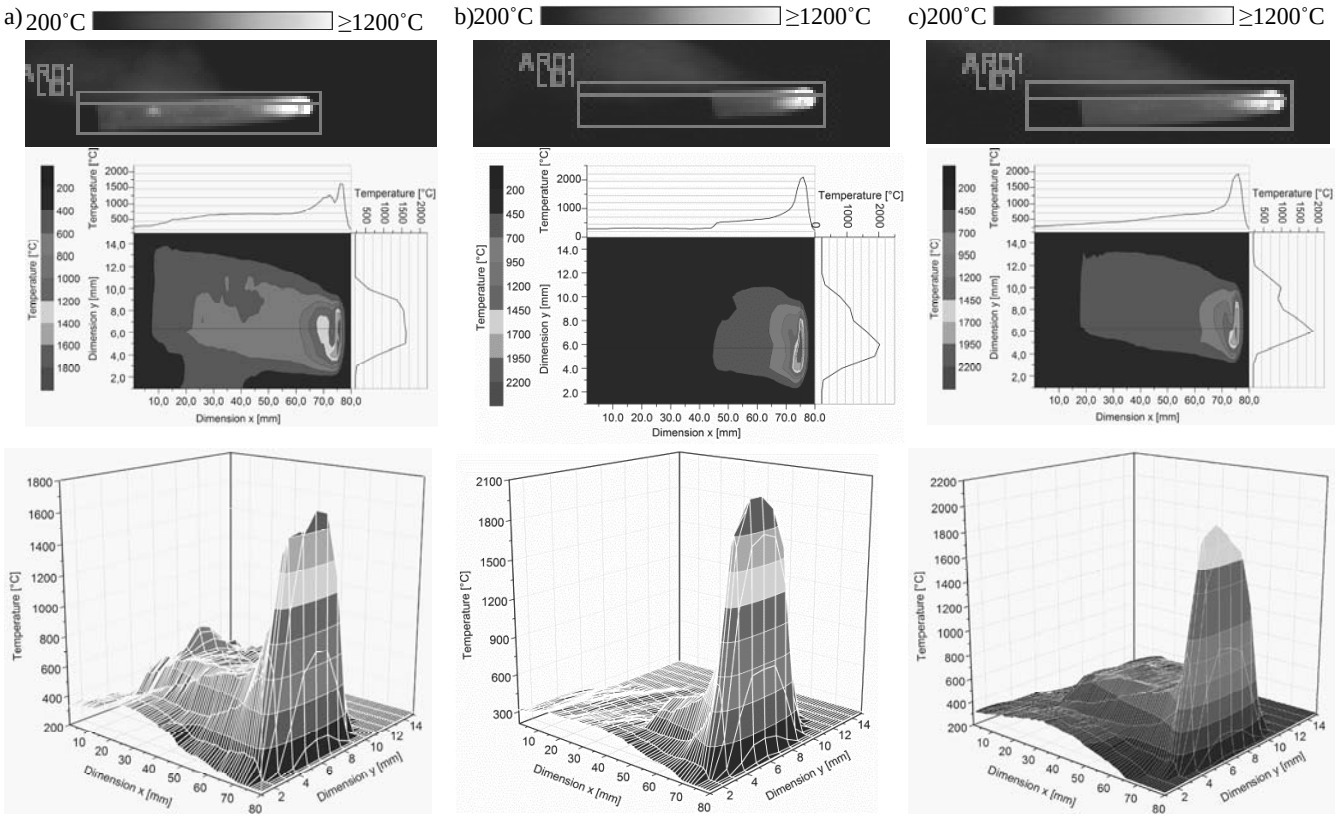

Fig. 7. Thermo-graphic image, temperature distribution in AR01 area and along X and Y axis after 5 s and the spatial distribution of temperature of molten pool during laser alloying with Si_3N_4 of: a) austenitic stainless steel X2CrNiMo17-12-2, b) ferritic stainless steel X6Cr13, c)duplex stainless steel X2CrNiMo22-8-2 at laser beam power of 2.1 kW, scanning speed rate 0.5 m/min.

Qualitative and quantitative temperature distribution on the sample surface of silicon nitride alloying performed using thermographic camera. Thermo camera it allows to recording the image presented distribution of temperature on the sample surface in execution sequence of laser process (Fig. 7). In order to ensure proper observation of the temperature distribution on the sample surface thermovision camera placed at a distance of 1 m from the observed point. Due to the high temperatures occurring during the surface treatment of an infrared camera was set to range in the range from 1200°C to 2000°C. Infrared spectra recorded by IR-camera allowed to determine the temperature of selected points and the temperature distribution on the sample surface as well as heating and cooling time of processed material, etc.. The analysis of thermo graphic images recorded during the laser alloying of

sintered stainless steels silicon nitride particle shows the smallest emission of infrared radiation field was observed for austenitic stainless steel X2CrNiMo17-12-2 and the largest one for ferritic, duplex for while it was in the middle. Sample infrared images shown in Figure 6. This phenomenon is closely related to the thermo-physical properties of alloyed steel and alloying powder dry as thermal conductivity, heat capacity and specific heat. During alloying in each case used the same Si_3N_4 powder therefore of its effect on the emissivity of by registered during the laser alloying process was always the same. The austenitic stainless steel is comparing ferritic and duplex alloy shows the lowest thermal conductivity, thus registered temperature of this sample was lower than for others alloys. Laser beam of high power diode laser HPDL is characterized very high local power density and high temperature gradient in the molten pool. Even when the laser beam power is on very low level of 0.7 kW the temperature of the substrate surface is on 1200°C. Although the surface temperature is very high the obtained structure and depth of remelting is not satisfaction. This situation can by explain by loss energy bring about water glass evaporation which is component of pre-coated paste Si_3N_4. When the water glass was evaporation and burned can be observed a dark smoke. This phenomenon a significantly impedes and distorts the data obtained by the thermo camera.

Simulations of physical phenomena occurring during the process of laser alloying of sintered stainless steel silicon nitride powder performed using the software Ansys 12.0. The simulations supply detailed data about size and shape the molten pool and the distribution of temperature in the volume sample. Computational model assumed different variants of application of powder and different parameters such as laser beam power and scan speed. It was assumed that the silicon nitride powder is supplied in paste form which is the mixture of water glass and Si_3N_4 as well as by two or three grooves with a depth-dependent model, 0.5 or 1 mm. During construction, the model assumes a nonlinear change in the density and thermo physical properties such as thermal conductivity and specific heat. The finite element mesh was created with the 20-noded thermal Solid90 elements. The element has a single degree of freedom, the temperature at each node. It was assumed ambient temperature and initial temperature of the sample rate of 293 K. The heating process was realized as a heat flux laser beam corresponding power of 0.7, 1.4 and 2.1 kW, while heat removal as radiation and convection of 800 J/kg. The latent heat effects were considered during solidification. The molten pool of liquid metal is a composite consisting of a sintered substrate material which is stainless steel and silicon nitride. No chemical reactions between the substrate and Si_3N_4 powder have been assumed. The sample is powder

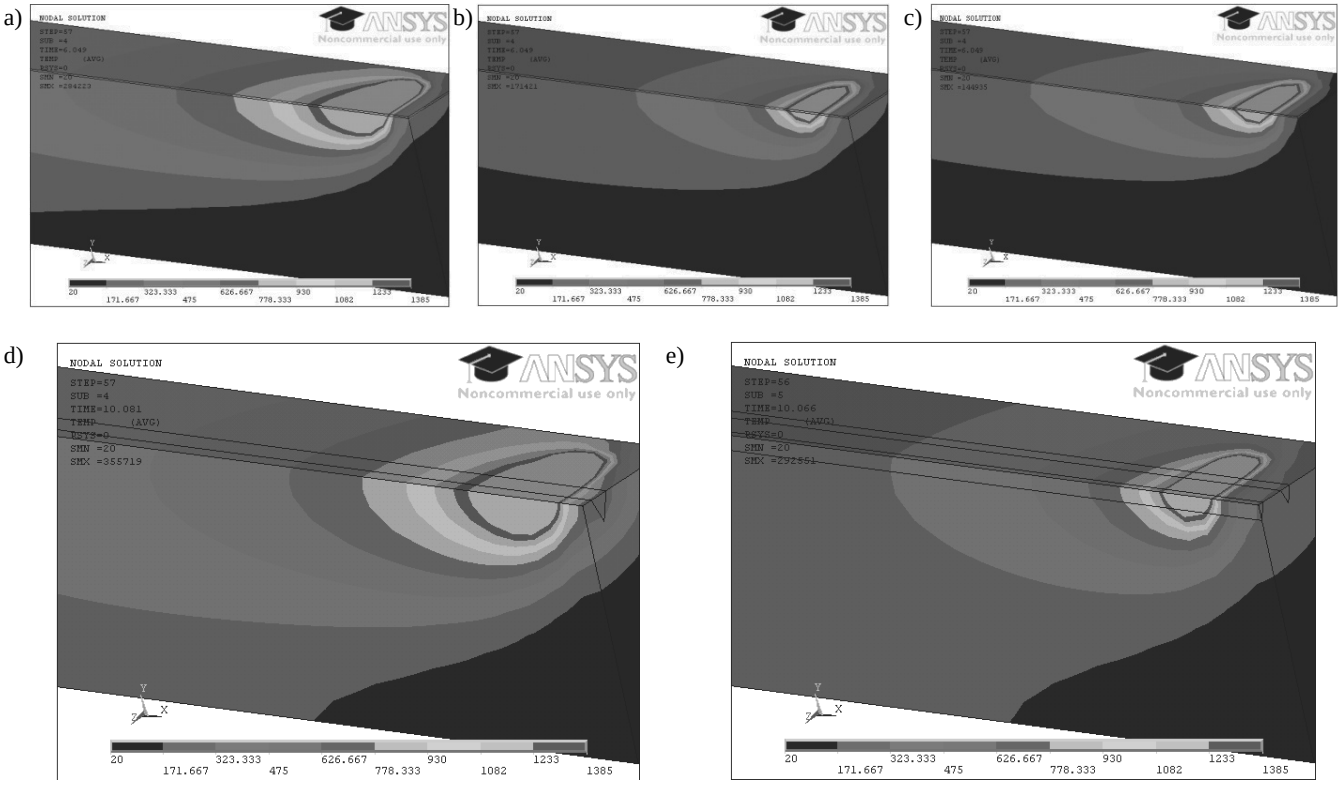

Fig. 8. The spatial distribution of temperature in a cross-section of sample during laser alloying with Si_3N_4 powder, a) austenitic stainless X2CrNiMo17-12-2, b) ferritic stainless steel X6Cr13, c) duplex stainless steel X2CrNiMo22-8-2; powder deposited as pre-coated paste, laser beam power 2.1 kW, scanning speed 0.5 m/min, d) austenitic stainless steel X2CrNiMo17-12-2, surface with 2 grooves, at laser beam power of 2.1 kW and scanning speed rate 0.3 m/min, e) ferritic stainless steel X6Cr13 surface with 3 grooves, at laser beam power of 2.1 kW and scanning speed rate 0.3 m/min.

coated and therefore the surface on which the laser beam falls is porous. For this reason, the high emissivity of 0.95 was assumed. The laser beam of dimensions 6.8 mm x 1.8 mm canter moves to the upper surface of which carry a silicon nitride powder at a constant speed of set up, depending on the model, 0.3 or 0.5 m/min. Numerical model of the process of laser alloying of steel sintered silicon nitride particle was used to determine the shape and size of the molten weld pool and to determine the temperature distribution and the volume of the sample and determine the depth of melting. Information about change temperature in time supplied by the simulations allows the reasoning of structural changes occurring during the process. The penetration depth was measured from the end of surface layer towards the depth basing on the temperature of melting metal, where as the final penetration depth was accepted the temperature melting temperature (Fig. 9). The possibly cladding material on the surface as well as shrinkage of molten pool during solidification was not taken into consideration. Basing on this assumption the penetration depth of alloyed layer can be easy calculated. Fig. 8 shows 3 different simulations dependent on elaborated 3-dimensional model.

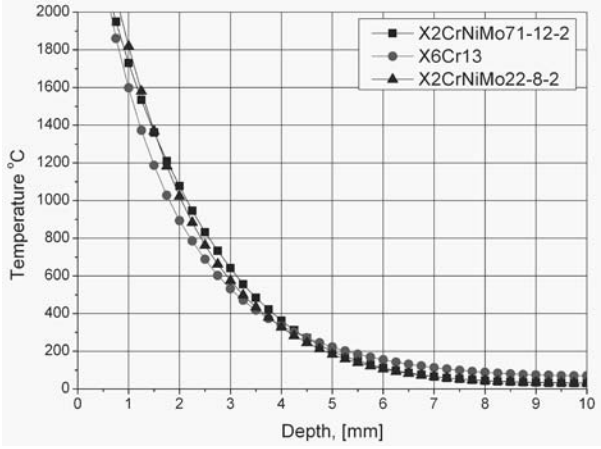

Fig. 9. The temperature changes in function of sample depths during laser alloying with Si_3N_4, austenitic stainless steel X2CrNiMo17-12-2, ferritic stainless steel X6Cr13 and duplex stainless steel X2CrNiMo22-8-2; laser beam power of 2.1 kW, scanning speed 0.3 m/min, with machined 2 grooves of 1.0 mm

Comparison of data obtained from the simulation with the values obtained experimentally showed significant compliance and confirmed the validity of adopted boundary conditions (Fig. 4). The shape and size of the molten pool diverged slightly from the results obtained experimentally. The heat flux input considered in simulation is only part of the mechanism for heating, thus the final shape of solidified molten pool will be depended of more variables. FEM Simulation showed the greatest depth of remelting the austenitic stainless X2CrNiMo17-12-2 and the smallest for ferritic stainless steel X6Cr13. Duplex stainless steel was classified in the middle. This is closely related to the thermo-physical properties of the substrate and the silicon nitride powder where the powder always exerts the same influence.

Figure 10 shows microstructure of austenitic saltiness steel with machined surface in the form of grooves then filled with Si_3N_4 powder. The microstructure in this case is composed of rectangular grains with visible alloying elements segregation on grain boundaries (Fig. 11).

a)

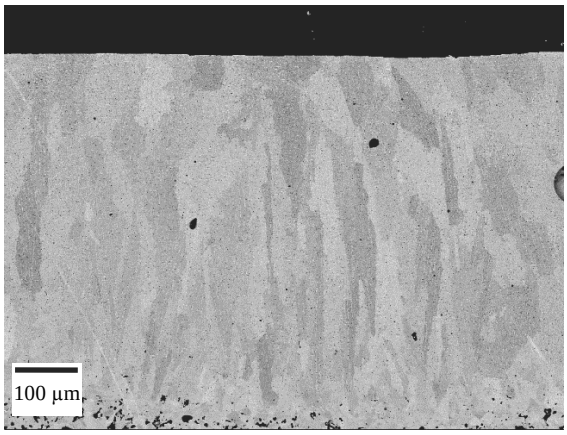

b)

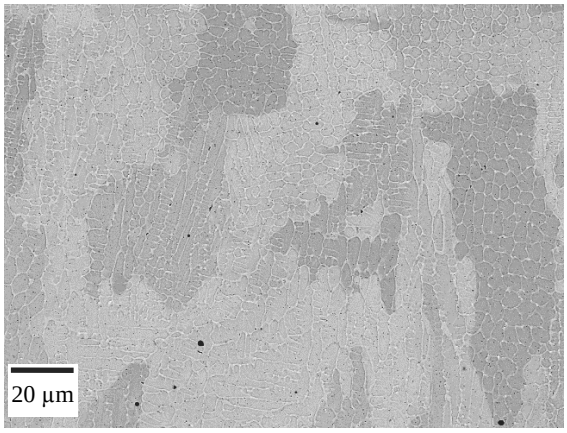

c)

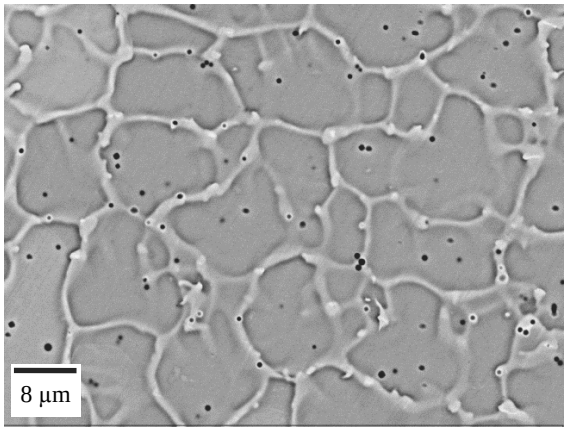

Fig. 10. Microstructure of austenitic stainless steel remelted with Si_3N_4 powder, surface with 3 grooves, at laser beam power of 2.1 kW and scanning speed rate 0.3 m/min, a) the edge of remelting zone, b, c) magnification in central zone

a)

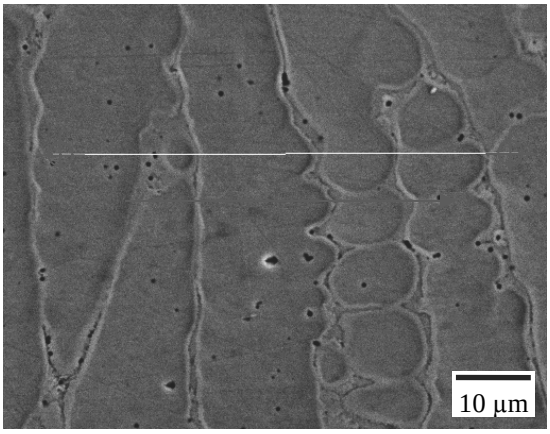

b)

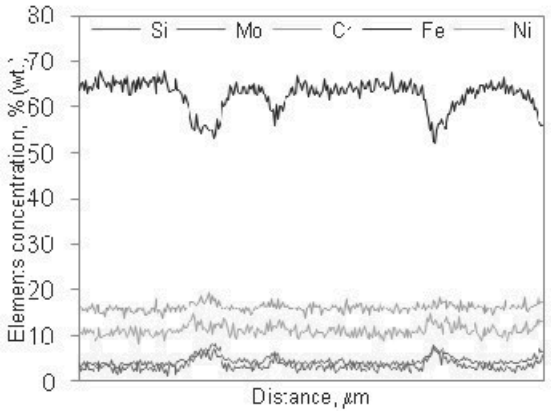

Fig. 11. Microstructure of austenitic stainless steel X2CrNiMo17-12-2 alloyed with Si_3N_4, 2 grooves 1.0mm, laser beam power 2.1 kW, scanning speed 0.3 m/min, a) microstructure b) EDS analysis of chemical composition according to Fig. (a)

Grains are oriented according to heat transfer direction, perpendicularly to the sample surface. Visible agglomerates of grains with various etching colours can be observed too. The X-ray analysis confirmed presence of pure austenitic microstructure when alloying with 2.1kW and no traces of Si_3N_4 that decomposed to Si and N and enriched steel matrix and stabilized austenitic phase (Fig. 12). Laser surface alloying with Si_3N_4 refined sintered stainless steel microstructure and enriched surface layer in Si (Fig. 13).

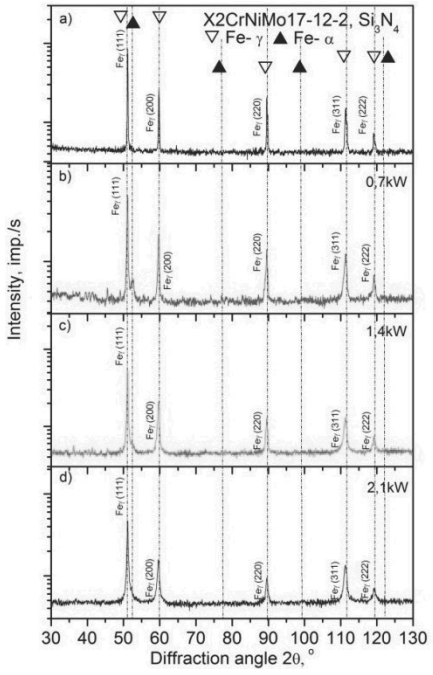

Fig. 12. The X-ray diffraction of sintered austenitic stainless steel X2CrNiMo17-12-2 alloyed with Si_3N_4, surface with 2 grooves 1.0 mm, at laser beam power of 2.1 kW and scanning speed rate 0.3 m/min

a)

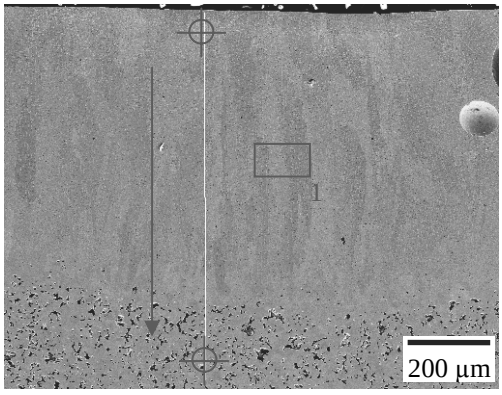

b)

Element	Chemical composition, %	
-	wt.	at.
Si	2.55	4.91
Cr	16.96	17.65
Fe	68.34	66.23
Ni	12.15	11.21

c)

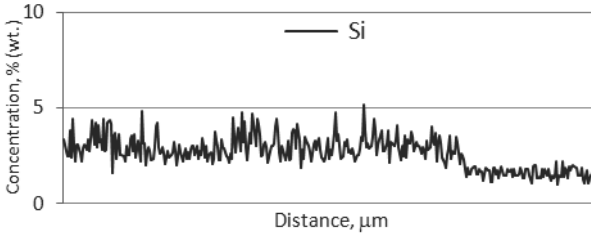

Fig. 13.Microstructure of austenitic stainless steel X2CrNiMo17-12-2 alloyed with Si_3N_4, 3 grooves 0.5 mm, laser beam power 2.1 kW, scanning speed 0.3 m/min, a) microstructure, b) EDS analysis of chemical composition according to zone 1 from Fig (a), c) linear change of chemical composition according to Fig (a)

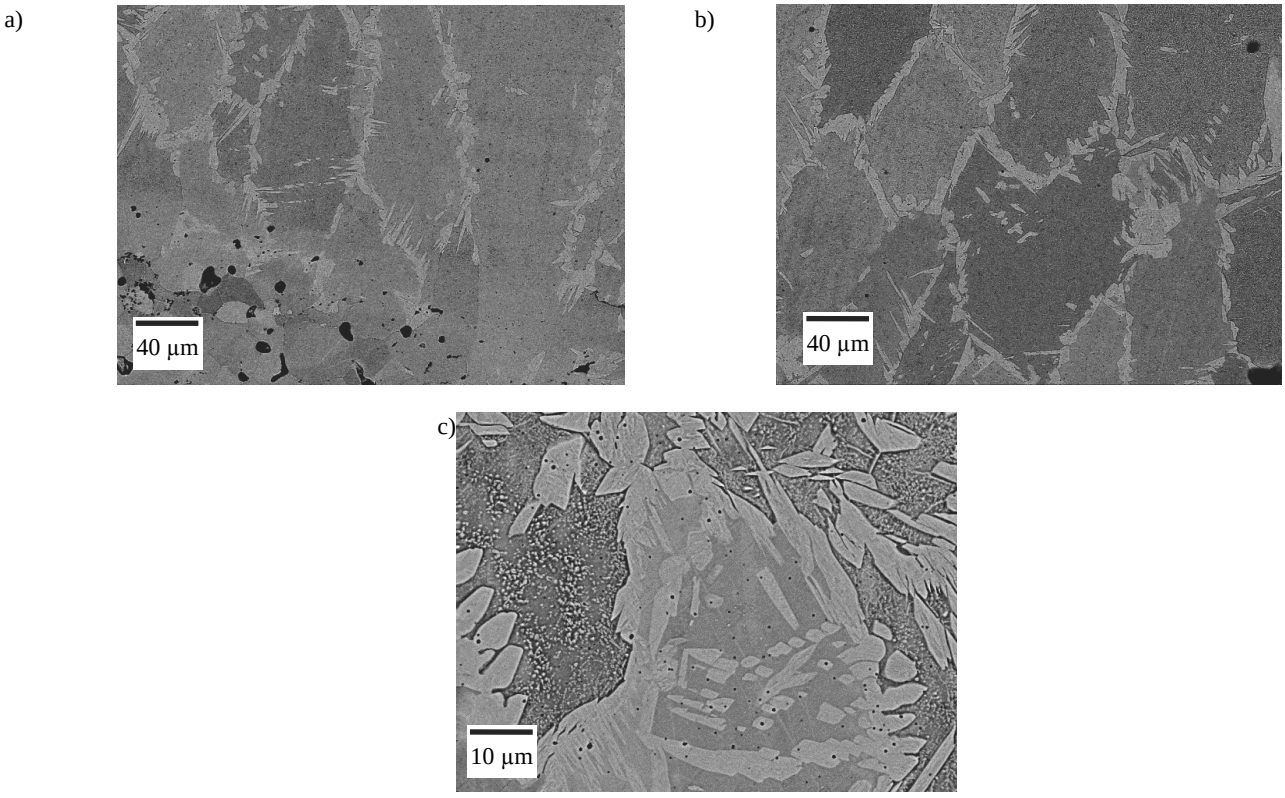

Fig. 14. Microstructure of ferritic stainless steel remelted with Si_3N_4 powder, surface with a, b) 3 grooves, c) 2 grooves, at laser beam power of 2.1 kW and scanning speed rate 0.3 m/min

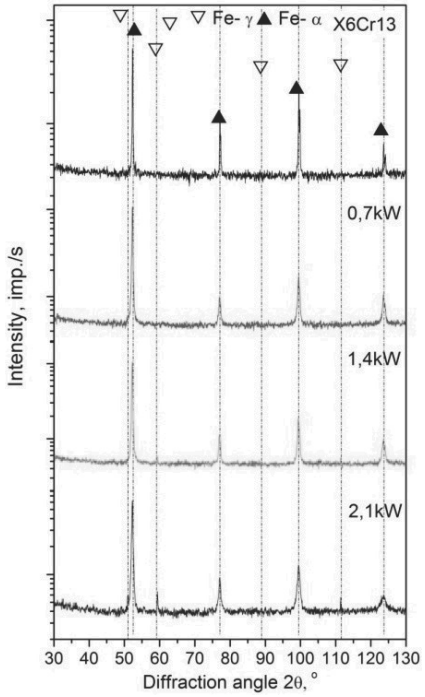

Fig. 15. The X-ray diffraction of sintered ferritic stainless steel X6Cr13 alloyed with Si_3N_4, surface with 2 grooves 1.0 mm, at laser beam power of 2.1 kW and scanning speed rate 0.3 m/min

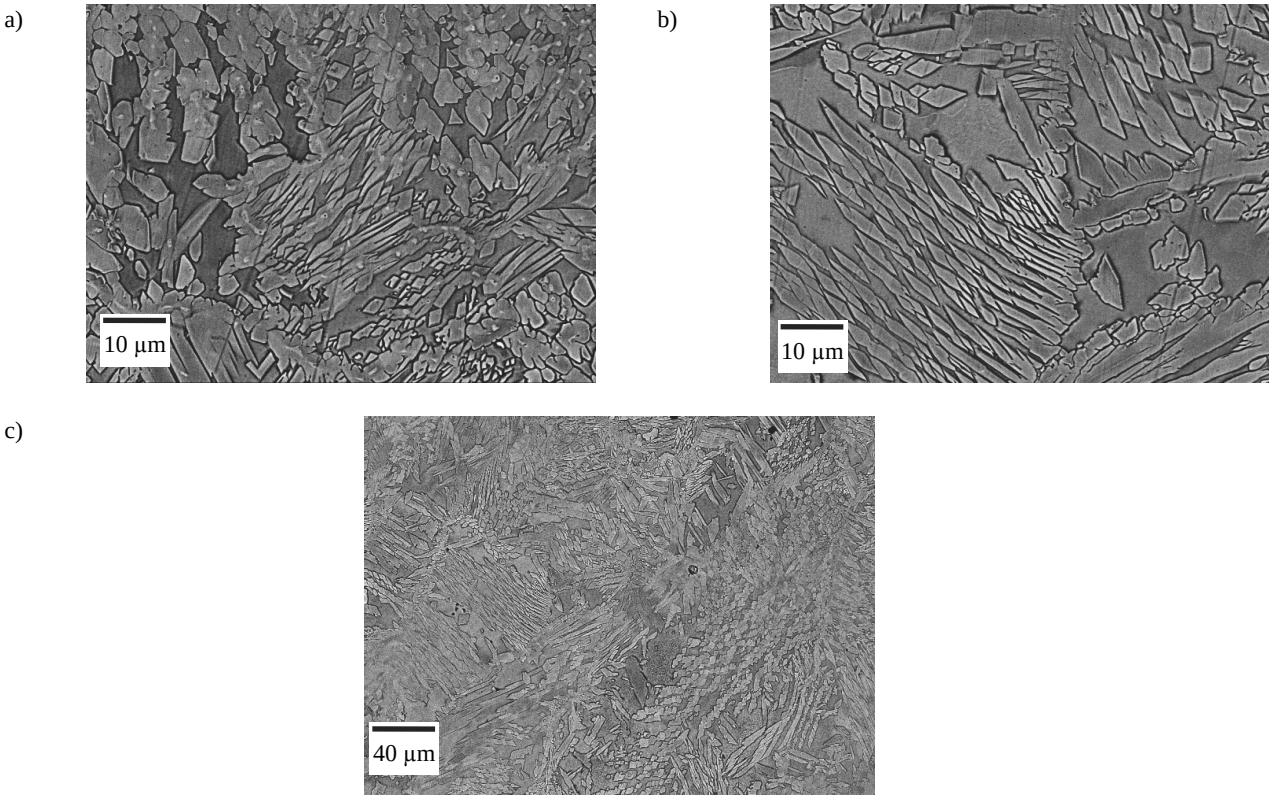

Fig. 16. Microstructure of duplex stainless steel remelted with Si_3N_4 powder, surface with 3 grooves, at laser beam power of 2.1 kW and scanning speed rate 0.3 m/min., a, b) the edge of remelting zone, c) magnification in central zone

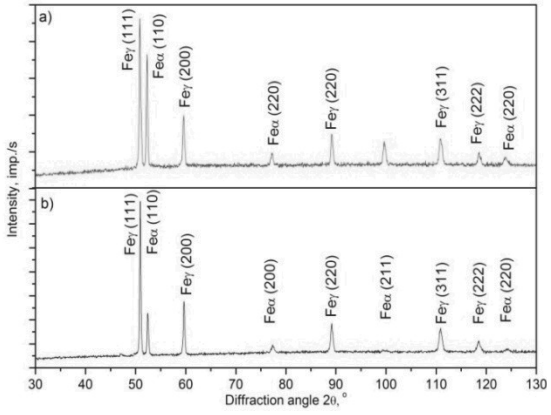

Fig. 17. The X-ray diffraction of sintered duplex stainless steel X2CrNiMo22-8-2 alloyed with Si_3N_4, samples with machined surface, alloyed at 2.1 kW and scanning speed of 0.3 m/min. a) 2 grooves 1.0 mm b) 3 grooves 0.5 mm

The similar effect of strong austenite stabilizer effect of N was observed in ferritic stainless steel alloyed with Si_3N_4powder (Fig. 14). The microstructure of alloyed zone become coarse grained ferritic matrix with precipitation of acicular austenite on grains boundaries. The zones of austenite precipitations are also located inside ferritic grains (Fig. 14c) where vary small austenitic grains have been precipitated. The ferritic matrix in these zones is also covered with micrometric precipitations, probably of nitrides. The x-ray analysis confirmed formation of duplex phase in alloyed surface layer when remelted at 2.1 kW (Fig. 15)

The duplex stainless steel (Fig. 16) after Si_3N_4 alloying shows very fine duplex microstructure, with the high quantity of fine austenitic grains. The rapid solidification in laser surface alloying process leading to ferrite content increase was balanced by austenite stabilizing effect of N from Si_3N_4, thus final duplex microstructure was well balanced in both phases. The x-ray analysis confirmed variable content of duplex microstructure and the increase of austenitic phase in samples with machined grooves (Fig. 17).

There are reasons for the increase in hardness with additions of Si_3N_4, because Si_3N_4 decomposes in the molten pool during laser irradiation, the concentration of nitrogen and silicon is increased. Both elements are solid solution hardeners, especially nitrogen. In case of pre-coated paste theoretically higher quantity of alloying material can be remelted thus the higher hardness could be obtained but unfortunately application of pre-coated paste for applied laser conditions does not provide satisfactory surface quality. The microhardness depth profile of samples with pre-coated paste (Figs. 18-20) shows that on case of 0.7kW surface microhardness was c.a. 150HV, while increasing laser beam power it was grooving to 250 $HV_{0.1}$ at the penetration dept of 0.2mm. The duplex stainless steel (Fig. 23) shows regular microhardness on the whole penetration depth of about 300 $HV_{0.1}$

at maximum laser beam power. The hardening effect of Si_3N_4 was strongest in case of ferritic stainless steel (Fig. 22) where microhardness increased to $450HV_{0.1}$ for 2.1 kW. Because of duplex microstructure, remelted layer is characterised by relatively high values of microhardness. The Si_3N_4 alloyed surfaces with machined grooves shows higher microhardness (Figs. 21-23), and more uniform distribution of obtained microhardness at the penetration depth. Beside studied variants of machined grooves (2 or 3) and their depth (0.5 or 1.0 mm), the layer with 2 grooves of 1.0 mm gives the same results as 3 groves of 0.5 mm (Fig. 23). Optimal results in term of surface quality, lack of cavities, uniform shape and smooth surface layer was obtained for 3 groves of 0.5 mm depth, what can be explained by high dilution ratio and therefore easier dissolution of the Si_3N_4 particle.

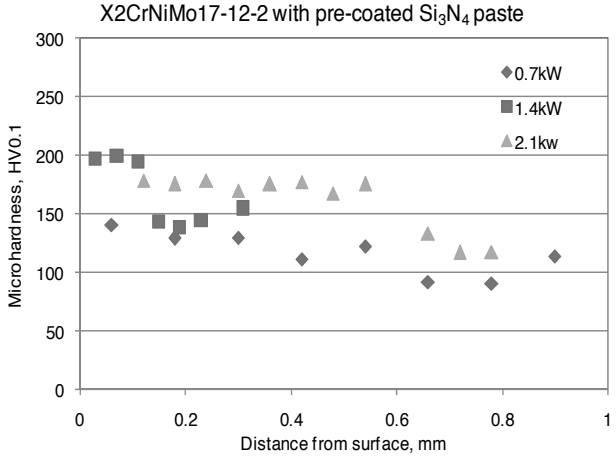

Fig. 18. Microhardness depth profile of austenitic stainless steels X2CrNiMo17-12-2 alloyed with Si_3N_4 as pre-coated paste at varied laser beam powers

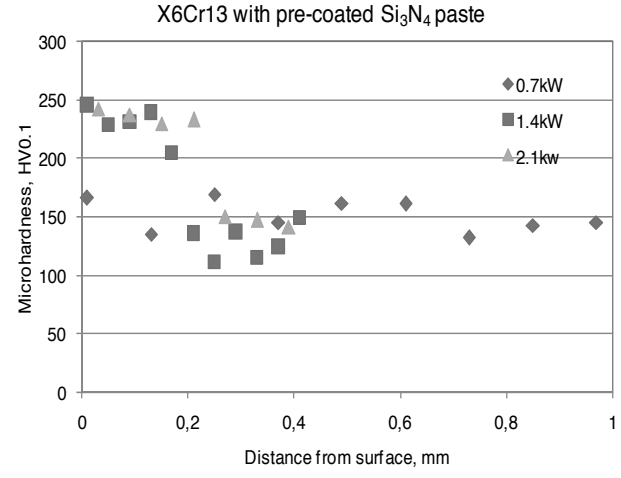

Fig. 19. Microhardness depth profile of ferritic stainless steels X6Cr13 alloyed with Si_3N_4 as pre-coated paste at varied laser beam powers

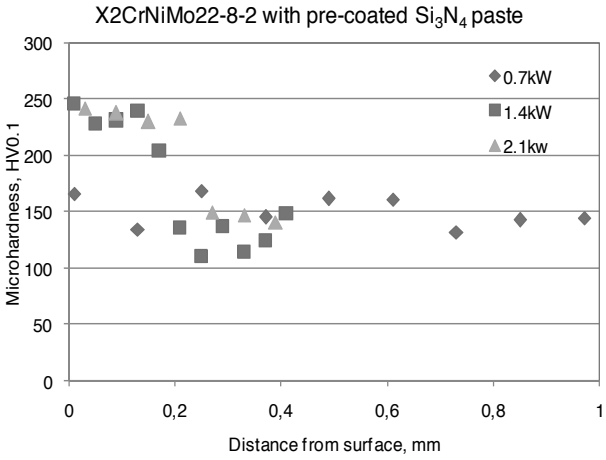

Fig. 20. Microhardness depth profile of duplex stainless steels X2CrNiMo22-8-2 alloyed with Si_3N_4 as pre-coated paste at varied laser beam powers

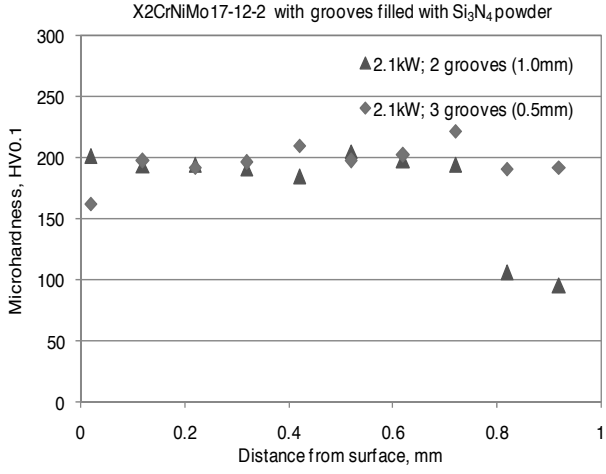

Fig. 21. Microhardness depth profile of austenitic stainless steels X2CrNiMo17-12-2 alloyed with Si_3N_4, surface with grooves at varied laser beam powers

The samples with machined 3 grooves shows higher wear resistance in respect to samples with 2 grooves (Fig. 24). Abrasion mechanism in this case seems to be in favour of a uniform microstructure obtained for 3 grooves of 0.5 mm than slightly harder surface but on less depth. In term of wear resistance the lower wear volume was obtained for alloyed duplex stainless steel. Improvement of wear resistance of alloyed duplex stainless steel is connected with increase of hardness due to ferrite content increase, fine microstructure formed by high cooling rates of laser processing. Increase of wear resistance can by explain by the fact that the silicon nitride dissolved in the molten pool during the laser process thus the increase concentration of silicon and nitrogen in remelted surface. The solution hardening by silicon and nitrogen influenced both hardness and wear resistance of laser alloyed stainless steels.

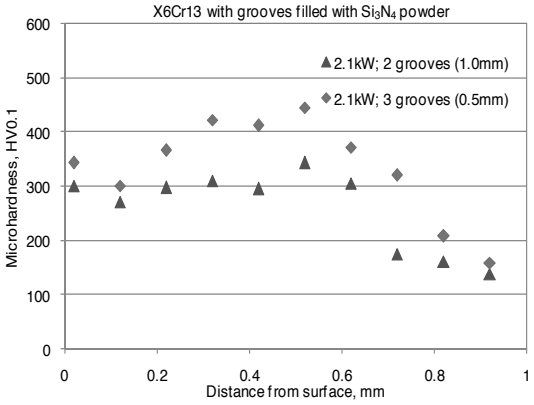

Fig. 22. Microhardness depth profile of ferritic stainless steels X6Cr13 alloyed with Si_3N_4, surface with grooves at varied laser beam powers

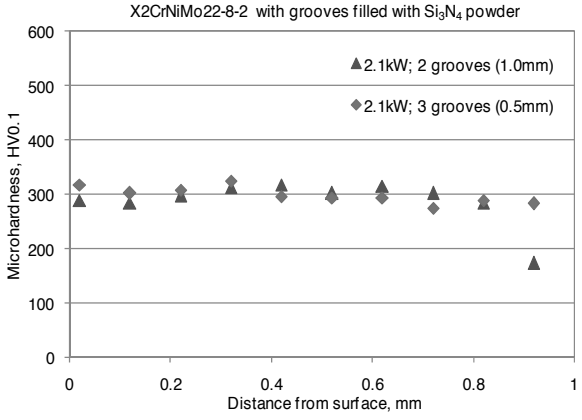

Fig. 23. Microhardness depth profile of duplex stainless steels X2CrNiMo22-8-2 alloyed with Si_3N_4, surface with grooves at varied laser beam powers

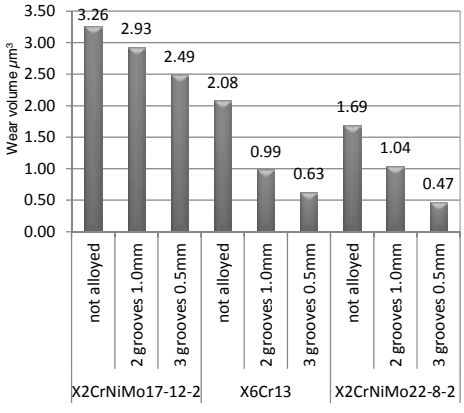

Fig. 24. Abrasive wear behaviour of laser alloyed Si_3N_4 layer (wear test: 5.0 mm diameter hardened steel ball, load 7.4 kN, reciprocal sliding movement, path of friction 7 mm, constant 9000 cycles)

4. Conclusions

Presented studies of laser surface alloying of sintered stainless steels with Si_3N_4 powder can be summarised as fallows:

a) The method of powder deposition on the sample surface plays an important role in achieved materials microstructures and properties. Generally surfaces prepared with pre-coated paste shows lover surface quality and possible success of alloying process than prepared as machined grooves of varied quantity and depth. The grooves machined in surface and then filled with alloyed powder creating opportunity of control the quantity of remelted material and the dilution ratio.

b) The penetration depth when alloyed with Si_3N_4 powder was c.a. 0.2 mm for ferritic and duplex stainless steel while for austenitic one it was as high as 0.9 mm. Proper penetration depth was achieved only when 1.4 and 2.1 kW of laser beam was applied. Surface with machined grooves proven his advantages in term of higher surface quality of alloyed layer than surface covered with pre-coated powder paste that acts as the barrier for laser radiation and lowers possible penetration depth. The penetration depth in this case was higher and ranged 0.5 to 1.2 mm.

c) The application of IR camera in the observation of laser surface alloying provide a lot of valuable information about temperature distribution on the sample surface during laser treatment and is helpful in understanding the occurring phenomena.

d) Comparison of penetration depth data obtained from the FEM simulation with the values obtained experimentally showed significant compliance and confirmed the validity of adopted FEM boundary conditions.

e) The microstructure of sintered stainless steels become enriched in silicon and nitrogen during laser irradiation and no traces of pure Si_3N_4 in microstructure have been found that decomposed to Si and N and stabilized austenitic phase.

f) The microstructure of austenitic stainless steel was composed of rectangular grains with visible alloying elements segregation on grain boundaries. The influence of strong austenite stabilizer effect of N was observed in ferritic stainless steel where microstructure become duplex one with coarse grained ferrite and precipitation of acicular austenite on grains boundaries. The duplex stainless steel shows very fine duplex microstructure, with the high quantity of fine austenitic grains. The rapid solidification in laser surface alloying process leading to ferrite content increase was balanced by austenite stabilizing effect of N from Si_3N_4, thus final duplex microstructure was well balanced in both phases.

g) The hardness increased with addition of Si_3N_4 due to strong solution hardening effect of nitrogen and silicon dissolved in the steel matrix during laser alloying. The hardening effect of Si_3N_4 was strongest in case of ferritic stainless steel where microhardness increased to $450HV_{0.1}$ for 2.1 kW. The duplex stainless steel shows the regular microhardness on the whole penetration depth.

h) Laser surface alloying with Si_3N_4 improved wear resistance of sintered stainless steels compared to not processed stainless steel as well as comparing layers prepared as machined grooves and surface with pre-coated paste.

Acknowledgements

The presented research was partially funded by the Polish Ministry of Science and Higher Education as a research project No. N507 470137.

References

[1] J.C. Betts, The direct laser deposition of AISI316 stainless steel and Cr_3C_2 powder, Journal of Materials Processing Technology 209 (2009) 5229-5238.
[2] F. Laroudie, C. Tassin, M. Pons, Hardening of 316L stainless steel by laser surface alloying, Journal of Materials Science 30 (1995) 3652-3657.
[3] D. Zhang, X. Zhang, Laser cladding of stainless steel with Ni-Cr_3C_2 and Ni-WC for improving erosive-corrosive wear performance, Surface and Coatings Technology 190 (2005) 212-217.
[4] C. Tassin, F. Laroudie, M. Pons, L. Lelait, Improvement of the wear resistance of 316L stainless steel by laser surface alloying, Surface and Coatings Technology 80 (1996) 207-210.
[5] J. Dutta Majumdar, I. Manna, Laser surface alloying of AISI304-stainless steel with molybdenum for improvement in pitting and erosion-corrosion resistance, Materials Science and Engineering A 267 (1999) 50-59.
[6] C.T. Kwok, F.T. Cheng, H.C. Man, Laser surface modification of UNS S31603 stainless steel, Part I, Microstructures and corrosion characteristics, Materials Science and Engineering A 290 (2000) 55-73.
[7] S. Zherebtsov, K. Meakawa, T. Hayashi, M. Futakawa, Laser surface alloying of SUS316 stainless steel with Al-Si, JSME International Journal A 48/4 (2005) 292-298.
[8] W.-T. Tsai, T.-H. Lai, J.-T. Lee, Laser surface alloying of stainless steel with silicon nitride. Materials Science Engineering A 183 (1994) 239-245.
[9] Ch.-K. Sha, H.-L. Tsai, Hardfacing characteristics of S42000 stainless steel powder with added silicon nitride using a CO_2 laser, Materials Characterization 52 (2004) 341-348.
[10] A. Lisiecki, A. Klimpel, Diode laser surface modification of Ti6Al4V alloy to improve erosion wear resistance, Archives of Materials Science and Engineering 32/1 (2008) 5-12.
[11] L.A. Dobrzański, S. Malara, T. Tański, Laser surface treatment of magnesium alloys with silicon carbide powder, Archives of Materials Science and Engineering 35/1 (2009) 54-60.
[12] L.A. Dobrzański, M. Bonek, E. Hajduczek, K. Labisz, M. Piec, E. Jonda, A. Polok, Structure and properties of laser alloyed gradient surface layers of the hot-work tool steel, Journal of Achievements in Materials and Manufacturing Engineering 31/2 (2008) 148-169.
[13] F. Yongquing, A.W. Batchelor, Laser alloying of aluminum alloy AA6061 with Ni and Cr, Part II, The effect of laser alloying on the fretting wear resistance, Surface and Coatings Technology 102 (2003) 468-471.
[14] A. Dudek, Z. Nitkiewicz, A. Górka, Structure and properties of laser alloyed surface layer, Journal of Achievements in Materials and Manufacturing Engineering 27/1 (2008) 75-78.
[15] S.-Z. Leea, K.-H. Zum Gahra, Laser-induced surface alloying of Al_2O_3 ceramics with ZrO_2-TiO_2 powders, Ceramics International 20/3 (1994) 147-157.
[16] A. Baron, W. Simka, G. Nawrat, D. Szewieczek, Electropolishing and chemical passivation of austenitic steel, Journal of Achievements in Materials and Manufacturing Engineering 31/2 (2008) 197-202.
[17] G. Niewielski, K. Radwański, D. Kuc, The impact of deformation on structural changes of the duplex steel, Journal of Achievements in Materials and Manufacturing Engineering 23/1 (2007) 31-34.
[18] W. Ozgowicz, A. Kurc, Structure and properties of forming austenitic X5CrNi18-9 stainless steel in a cold working, Journal of Achievements in Materials and Manufacturing Engineering 33/1 (2009) 19-26.
[19] L.A. Dobrzański, A. Zarychta, M. Ligarski, Phase transformations during heat treatment of W-Mo-V 11-2-2 type high-speed steels with increased contents of Si and Nb or Ti, Journal of Materials Processing Technology 53/1-2 (1995) 109-120.
[20] L.A. Dobrzański, A. Drygała, K. Gołombek, P. Panek, E. Bielańska, P. Zięba, Laser surface treatment of multicrystalline silicon for enhancing optical properties, Journal of Materials Processing Technology 201/1-3 (2008) 291-296.
[21] L.A. Dobrzański, M. Bonek, A. Klimpel, A. Lisiecki, Surface-Layer's Structure of X40CrMoV5-1 Steel Remelted and/or WC Alloyed with HPDL Laser, Materials Science Forum 437-438 (2003) 69-72
[22] Z. Brytan, L.A. Dobrzański, M. Actis Grande, M. Rosso, Characteristics of vacuum sintered stainless steels, Journal of Achievements in Materials and Manufacturing Engineering 33/2 (2009) 126-134.
[23] Z. Brytan, M. Actis Grande, M. Rosso, R. Bidulský, L.A. Dobrzański, Stainless steels sintered form the mixture of prealloyed stainless steel and alloying element powders, Materials Science Forum 672 (2011) 165-170.
[24] Z. Brytan, L.A. Dobrzański, M. Actis Grande, M. Rosso, The influence of sintering time on the properties of PM duplex stainless steel, Journal of Achievements in Materials and Manufacturing Engineering 37/2 (2009) 387-396.
[25] Z. Brytan, M. Bonek, L.A. Dobrzański, D. Ugues, M. Actis Grande, The laser surface remelting of austenitic stainless steel, Materials Science Forum 654-656 (2010) 2511-2514.
[26] Z. Brytan, M. Bonek, L.A. Dobrzański, W. Pakieła, Surface Layer Properties of Sintered Ferritic Stainless Steel Remelted and Alloyed with FeNi and Ni by HPDL Laser, Advanced Materials Research 291-294 (2011) 1425-1428.